

# A Quantum Approximate Optimization Method For Finding Hadamard Matrices

Andriyan Bayu Suksmono

The School of Electrical Engineering and Informatics  
Institut Teknologi Bandung, Indonesia

August 16, 2024

## Abstract

Finding a Hadamard matrix of a specific order using a quantum computer can lead to a demonstration of practical quantum advantage. Earlier efforts using a quantum annealer were impeded by the limitations of the present quantum resource and its capability to implement high order interaction terms, which for an  $M$ -order matrix will grow by  $O(M^2)$ . In this paper, we propose a novel qubit-efficient method by implementing the Hadamard matrix searching algorithm on a universal quantum computer. We achieve this by employing the Quantum Approximate Optimization Algorithm (QAOA). Since high order interaction terms that are implemented on a gate-based quantum computer do not need ancillary qubits, the proposed method reduces the required number of qubits into  $O(M)$ . We present the formulation of the method, construction of corresponding quantum circuits, and experiment results in both a quantum simulator and a real gate-based quantum computer. The experiments successfully found the Baumert-Hall type Hadamard matrices up to 132. These results motivate further efforts to discover previously unknown Hadamard matrices and a prospect to ultimately demonstrate practical quantum advantages.

**Keywords**— quantum computing, hard problems, hadamard matrix, quantum annealing, QAOA, quantum approximate optimization algorithm, optimization, quantum advantage, NISQ, Noisy Intermediate Scale Quantum

## 1 Introduction

Quantum computing is considered reaching an important milestone in 2019 when Google's quantum computer outperformed a classical supercomputer in doing a specific computational task; i.e. random quantum circuit sampling [1]. Whereas a classical super computer needed about 10,000 years, the 53 qubits Sycamore took around 200 seconds to finish the task, thanks to its capability in representing  $2^{53} \approx 10^{16}$  computational state-space. The next stage after this milestone, according to this paper, is showing the capability of a quantum computer to solve a more valuable computing applications. Although at present time ideal fault-tolerant and sufficient number of qubits for implementing quantum algorithms has not been achieved; i.e an era that is called NISQ (Noisy Intermediate Scale Quantum), various efforts to this direction have been initiated. One of the methods for using the NISQ devices for solving a real-world computing problem is by employing a hybrid classical-quantum algorithm, such as the QAOA (Quantum Approximate Optimization Algorithm) that was proposed by Farhi et.al. [2].

To this day, various theoretical research, improvements, and explorations on possible applications of the QAOA have been conducted by researchers. In [3], Boulebname et.al. reported

their investigation on the performance of QAOA in sampling low-energy states for protein folding problems. Their results indicate that, whereas simpler problems give promising results, a more complex one that required a deeper quantum circuit only comparable to that of random sampling. Considering the close relationship with the adiabatic algorithm, a study on choosing the QAOA initial state in a constrained portfolio optimization problem was reported by He et al. They found that the best initial state is the ground state of the mixing Hamiltonian [4]. Improvement to the QAOA performance is also actively being explored. A double adaptive-region Bayesian optimization for QAOA which indicates a better performance in terms of speed, accuracy, and stability, compared to conventional optimizer is reported in [5]. On the application side, a data-driven QAOA for distributed energy resource problem in power systems is reported by Jing et.al [6].

Another significant result on the usage of NISQ devices is the demonstration of quantum utility before fault tolerance, which was recently conducted by IBM researchers [7]. This results bring hopes on the implementation and demonstration of quantum advantage for real-world applications. In line with this spirit, we propose a hard problem of discovering a particular discrete structure—which is a specific order of Hadamard matrix, as a potential instance of such practical applications and use QAOA for implementation in gate-based quantum computers.

A Hadamard matrix (H-matrix) is an orthogonal binary matrices with various scientific and engineering applications [8, 9, 10, 11]. An  $M$ -order H-matrix exists only when  $M$  equal to 1, 2, and multiples of 4. The converse, that for every positive integer  $k$  there is a Hadamard matrix of order  $4k$  is also believed to be true [12, 11], which is the well known Hadamard matrix conjecture. When  $M = 2^n$ , for a non-negative integer  $n$ , the H-matrix can be constructed easily by Sylvester method [12]. Construction of H-matrix with other values of  $M = 4k$  has also been developed, among others are the methods by Paley [13], Williamson [14], Baumert-Hall [15], and Turyn [16]. More recently, co-cyclic techniques are developed by Delauney-Horadam [17, 18, 19], and Alvarez et al. [20]. Nevertheless, not all of Hadamard matrices are neither easily constructed nor discovered. The latest one is a H-matrix of order 428, which was found by Kharaghani and Tayfeh-Rezaie [21]. Up to this day, for order  $M < 1000$ , the H-matrices of order 668, 716, 892 have neither been discovered nor proven to exist. Our previous study indicates that, by using currently known methods, present-day (classical) computing resources are insufficient to find those matrices in practical time.

In principle, an  $M$ -order H-matrix can be found or proven to be non-exist, using an exhaustive method by checking all possible  $+1/-1$  combinations of its  $M \times M$  entries. However, when the value of  $M$  is sufficiently large, it is computationally impractical because the number of orthogonality test to be performed will grow exponentially as  $O(2^{M \times M})$ , although the test itself can be done in a polynomial time. Regarding this issue, we have developed some methods based on SA (Simulated Annealing), SQA (Simulated Quantum Annealing) [22], and QA (Quantum Annealing) [23, 24]. The latest one of our method have been implemented on a quantum annealer; which is the D-Wave quantum computer, and we successfully found a few H-matrix of order more than one hundred [24]. Although the number of qubits in present days quantum annealer is more than 5,000, the necessity of the ancillary qubits to represent more than 2-body interaction hinders implementation to find higher-order H-matrices. We have estimated that the implementation of the method for finding a 668-order H-matrix needs at least 15,400 physical qubits [24].

A tentative way to pursue this task is by developing a qubit-efficient method. This paper deals with this idea, i.e., instead of using the quantum annealer, we propose to employ a universal gate quantum computer for implementing the method. An almost straight forward extension for the previous method is by formulating the problem as an instance of the QAOA (Quantum Approximate Optimization Algorithm) method [2]. In a universal gate quantum computer, the number of interaction in the Hamiltonian terms is not limited to only the 2-body interaction, as in the quantum annealer case. The extra ancillary qubits for the implementation of high order interacting terms is not required when we use such universal quantum computer.

## 2 Methods

In this paper, we use two kinds of binary variables, which are a Boolean variable whose value is either 0 or 1 and a spin variable whose value is either  $-1$  or  $+1$ . The value of 0 in the Boolean variable will be mapped to  $+1$  in the spin variable and vice versa, whereas 1 of the Boolean's will be mapped into  $-1$  in the spin variable and vice versa. As an example, a (Boolean) bit string such as 010110 is mapped into a (spin) vector  $[1, -1, 1, -1, -1, 1]$ . Both of the Boolean and spin variables will be used interchangeably according to the context of discussion.

### 2.1 Finding H-Matrices as a Binary Optimization Problem

A direct method to find an  $M$ -order a H-matrix, i.e. a binary orthogonal matrix of size  $M \times M$ , can be done by checking the orthogonality condition of all possible binary matrices  $B = [b_{m,n}]$ , where  $b_{m,n} \in \{-1, +1\}$ . The orthogonality test can be formulated as a cost function  $C_D(B)$ , which is the sum of the squared off-diagonal elements of an indicator matrix  $D = [d_{m,n}] = B^T B$ , which can be expressed by,

$$C_D(B) = C(b_{m,n}) = \sum_{m=0}^{M-1} \sum_{n=0}^{M-1} (d_{m,n} - I_{m,n})^2 \quad (1)$$

where  $I$  is an  $M \times M$  identity matrix. When  $C_D(B) = 0$ , then the matrix  $B$  is orthogonal and therefore it is a H-matrix; otherwise it is not. It is not an efficient method due to the number of binary matrices to check is  $2^{M \times M}$ .

A more efficient way of finding the H-matrix is by employing the Williamson/Baumert-Hall [12] or the Turyn methods [16, 21, 25]. We also have developed optimization based methods that employs quantum computers to find the H-matrix, which are the QA (Quantum Annealing) direct method by representing each entries as a binary variable [23], the QA Williamson/Baumert-Hall method, and the QA Turyn method [24]. Whereas the number of variables in the QA direct method grows with the order  $M$  by  $O(M \times M)$ , the QA Williamson/Baumert-Hall and the QA Turyn methods only grows by  $O(M)$ , which is more efficient in term of the number of the variables. However, when it is implemented on the present day quantum annealer, such as the D-Wave, not only each variable should be represented by a qubit, but additional *ancillary* qubits are also required for representing 3-body and 4-body terms. Accordingly, the required number of qubits grows with the order of the matrix by  $O(M \times M)$ . Since the qubit is one of the most valuable resources in quantum computing, a more efficient method that can reduce the number of qubits is highly desired.

In the Williamson based method [24], we seek for a binary  $\{-1, +1\}$  vector

$$\vec{s} = [s_0, s_1, \dots, s_n, \dots, s_{N-1}] \quad (2)$$

where  $s_n \in \{-1, +1\}$ , that minimize a Williamson cost function  $C_W(\vec{s})$  that is given by,

$$C_W(\vec{s}) = \sum_{i=0}^{K-1} \sum_{j=0}^{K-1} (v_{i,j}(\vec{s}) - 4k\delta_{i,j})^2 \quad (3)$$

In this equation,  $v_{i,j}(\vec{s})$  is the elements of matrix  $V$  that is constructed from four sub-matrices  $A, B, C$ , and  $D$  of dimension  $K \times K$ ; that is,

$$V = A^T A + B^T B + C^T C + D^T D \quad (4)$$

where  $V = V(\vec{s})$ ,  $A = A(\vec{s})$ ,  $B = B(\vec{s})$ ,  $C = C(\vec{s})$ ,  $D = D(\vec{s})$  are sub-matrices whose elements include some particular elements of the vector  $\vec{s}$ . When  $C_W(\vec{s}) = 0$ , then the matrix  $H$  of size  $4K \times 4K$  given by the following block matrix

$$H = \begin{pmatrix} A & B & C & D \\ -B & A & -D & C \\ -C & D & A & -B \\ -D & -C & B & A \end{pmatrix} \quad (5)$$

is Hadamard [12]. A larger Baumert-Hall matrix can also be constructed from the same  $\{A, B, C, D\}$  submatrices [12]. We will call the binary representation of vector  $\vec{s}$  given in Eq. (2) that minimize Eq.(3) as a Williamson/Baumert-Hall string or a *WBH-string*.

In the Turyn based method, we also seek for a vector  $\vec{s} = [s_0, s_1, \dots, s_{N-1}]$  like in Eq.(2) that minimize a Turyn cost function  $C_T(\vec{s})$  given by

$$C_T(\vec{s}) = \sum_{r>1} (N_{X(\vec{s})}(r) + N_{Y(\vec{s})}(r) + 2N_{Z(\vec{s})}(r) + 2N_{W(\vec{s})}(r))^2 \quad (6)$$

where  $N_{X(\vec{s})}(r), N_{Y(\vec{s})}(r), N_{Z(\vec{s})}(r), N_{W(\vec{s})}(r)$  are non-periodic auto-correlation functions of sequences  $X(\vec{s}), Y(\vec{s}), Z(\vec{s}), W(\vec{s})$ , respectively, which are calculated at lagged  $r$ . Note that for a sequence  $X = [x_0, x_1, \dots, x_{N-1}]$ , the non-periodic auto-correlation function is given by [21, 25],

$$N_X(r) = \begin{cases} \sum_{n=0}^{N-1-r} x_n x_{n+r} & , 0 \leq r \leq N-1 \\ 0 & , r \geq N \end{cases} \quad (7)$$

Similarly as in the previous case, we will call the bianry representation of vector  $\vec{s}$  that makes  $C_T(\vec{s}) = 0$  as a Turyn string or *T-string*. In this paper, since the number of variables can be very large, the computation of the cost functions  $C_W(\vec{s})$  and  $C_T(\vec{s})$  and its corresponding Hamiltonian expression are performed by symbolic computing.

## 2.2 QAOA Formulation of H-matrix Searching Problem

The QAOA is a hybrid classical-quantum algorithm proposed by Farhi et.al [2]. It is a solution for near-term quantum computing, which can be implemented on a Noisy Intermediate-Scale Quantum (NISQ) device; i.e., a quantum computer with limited number of qubits, connectivity, gate errors, and short coherence times. A typical  $N$ -bit and  $M$ -clause combinatorial optimization problem addressed by the QAOA can be formulated as follows. Consider an  $N$ -length bit string  $\vec{b} = b_0 b_1 \dots b_{N-1}$  and let  $C(\vec{b})$  be a cost or an objective function given by the following expression

$$C(\vec{b}) = \sum_{m=0}^{M-1} C_m(\vec{b}) \quad (8)$$

The value of  $C_m(\vec{b})$  is equal to 1 if  $\vec{b}$  satisfies the clause  $C_m$ , otherwise it is 0. When  $C$  is the maximum value of Eq. (8), the approximation means that we seek for a bit string  $\vec{b}$  where  $C(\vec{b})$  is close to  $C$ .

For applying the QAOA to the H-matrix searching problem, we change the Boolean vector  $\vec{b}$  in Eq. (8) into into its spin vector representation  $\vec{s} = [s_0, s_1, \dots, s_M]$ , while the maximization is recast as minimization. We can restate the previous approximation problem into finding a vector  $\vec{s}$  that minimize a non-negative cost function given by

$$C(\vec{s}) = \sum_{m=0}^{M-1} C_m(\vec{s}) \quad (9)$$

Then, the approximation means that we seek for a bit string  $\vec{b}$  corresponding to the vector  $\vec{s}$  that makes  $C(\vec{s})$  close to zero.

In the QAOA method, we have a Hamiltonian  $H$  that consists of a *problem Hamiltonian*  $H_C$  and a *mixer Hamiltonian*  $H_B$ ,

$$H = H_C + H_B \quad (10)$$

Then, we construct a quantum circuit to perform the following unitary transform

$$U(\gamma, \beta) = e^{-i\beta_P H_B} e^{-i\gamma_P H_C} e^{-i\beta_{P-1} H_B} e^{-i\gamma_{P-1} H_C} \dots e^{-i\beta_p H_B} e^{-i\gamma_p H_C} \dots e^{-i\beta_1 H_B} e^{-i\gamma_1 H_C} \quad (11)$$

where

$$H_B = \sum_j b_j \hat{\sigma}_j^x \quad (12)$$

and

$$H_C = \sum_{j,k,\dots,m,n} c_{jk\dots mn} \hat{\sigma}_j^z \hat{\sigma}_k^z \dots \hat{\sigma}_m^z \hat{\sigma}_n^z \quad (13)$$

In these equations,  $P$  is the number of layers (Trotter slice),  $\gamma_p$  and  $\beta_p$  are (angle) parameters at layer  $p$ ,  $b_j$  and  $c_{j,k,\dots,m,n}$  are constants, whereas  $\hat{\sigma}_j^x$  and  $\hat{\sigma}_j^z$  are the  $j^{th}$  spin/Pauli matrices in  $x$  and  $z$ -directions, respectively.

The term expressed by the product of  $n$  Pauli matrices  $\hat{\sigma}_0^z \hat{\sigma}_1^z \cdots \hat{\sigma}_{n-1}^z$  in Eq.(13) is called an  $n$ -body interaction term. In the Hadamard Searching Problem (H-SEARCH), there are only up to 4-body interaction in the Hamiltonian, so that generally  $H_C$  can be expressed by

$$H_C = \sum_j c_j \hat{\sigma}_j^z + \sum_{j,k} c_{jk} \hat{\sigma}_j^z \hat{\sigma}_k^z + \sum_{j,k,m} c_{jkm} \hat{\sigma}_j^z \hat{\sigma}_k^z \hat{\sigma}_m^z + \sum_{j,k,m,n} c_{jkmn} \hat{\sigma}_j^z \hat{\sigma}_k^z \hat{\sigma}_m^z \hat{\sigma}_n^z \quad (14)$$

The construction of quantum circuits related to each term of the  $n$ -body interactions in Eq.(14) are done as follows.

Consider a general problem Hamiltonian given by Eq. (14). By using Eq.(11), the unitary for of a single layer problem's Hamiltonian can be expressed by

$$U(\gamma) = \prod_j e^{-i\gamma c_j \hat{\sigma}_j^z} \prod_{j,k} e^{-i\gamma c_{jk} \hat{\sigma}_j^z \hat{\sigma}_k^z} \prod_{j,k,m} e^{-i\gamma c_{jkm} \hat{\sigma}_j^z \hat{\sigma}_k^z \hat{\sigma}_m^z} \prod_{j,k,m,n} e^{-i\gamma c_{jkmn} \hat{\sigma}_j^z \hat{\sigma}_k^z \hat{\sigma}_m^z \hat{\sigma}_n^z} \quad (15)$$

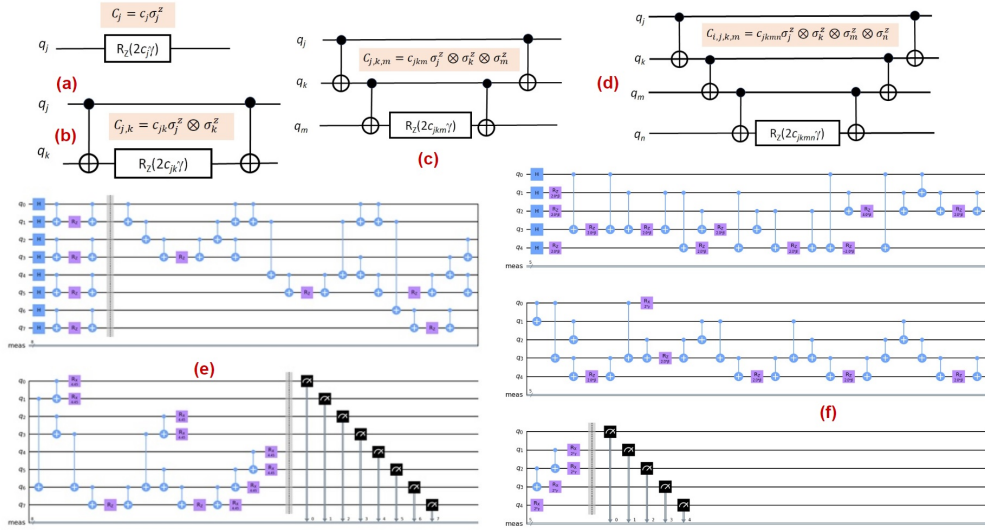


Figure 1: Elementary and QAOA-Implemented Quantum Circuits: (a) 1-body term, (b) 2-body term, (c) 3-body term, (d) 4-body-term, (e) a 1-layer quantum for 12-order QAOA-Williamson/Baumert-Hall method, and (f) a 1-layer quantum circuit of 44-order QAOA-Turyn method.

We can represent the exponentiation of  $\hat{\sigma}^z$  as a rotation in  $z$ -direction,  $R_Z(\dots)$ , as follows

$$U(\gamma) = e^{-i\gamma \hat{\sigma}^z} = e^{-i\gamma \begin{pmatrix} 1 & 0 \\ 0 & -1 \end{pmatrix}} = \begin{pmatrix} e^{-i\gamma} & 0 \\ 0 & e^{i\gamma} \end{pmatrix} = R_Z(2\gamma)$$

By substitution of  $\gamma' = c_j \gamma$ , we have

$$U(c_j \gamma) = U(\gamma') = e^{-c_j \gamma \hat{\sigma}^z} = R_Z(2c_j \gamma)$$

The first term of the product in Eq.(15), considering there are  $N$  qubits to be rotated, can be expanded into

$$\prod_j e^{-ic_j \gamma \hat{\sigma}_j^z} = \begin{pmatrix} e^{-ic_0 \gamma} & 0 \\ 0 & e^{ic_0 \gamma} \end{pmatrix} \otimes \begin{pmatrix} e^{-ic_1 \gamma} & 0 \\ 0 & e^{ic_1 \gamma} \end{pmatrix} \otimes \cdots \otimes \begin{pmatrix} e^{-ic_{N-1} \gamma} & 0 \\ 0 & e^{ic_{N-1} \gamma} \end{pmatrix}$$

or, by denoting the  $Z$  rotation on qubit  $n$  as  $R_{Z_n}(\dots)$ , we can write

$$\prod_j e^{-ic_j \sigma_j^z} = R_{Z_0}(2c_0\gamma) \otimes R_{Z_1}(2c_1\gamma) \otimes \cdots \otimes R_{Z_{N-1}}(2c_{N-1}\gamma)$$

The products in Eq.(15) can be interpreted as a cascaded operations. Then, a 1-body terms in the Hamiltonian that is expressed by  $H_{C1} = \sum_j c_j \hat{\sigma}_j^z$  can be implemented as a quantum circuit given by Fig. 1.(a), which is a  $Z$ -rotation of angle  $2c_j\gamma$ . Higher order terms, which are 2-,3-, and 4- body interacting terms, can also be treated similarly, but with a different elementary circuits in the cascaded block.

The quantum circuits implementation of the  $k$ -body interactions displayed in Fig. 1 (b), (c), and (d) are adopted from Nielsen-Chuang [26], Seeley [27], and Setia [28]. A 2-body terms in the Hamiltonian  $H_{C2} = \sum_{j < k} c_{jk} \hat{\sigma}_j^z \hat{\sigma}_k^z$  has a corresponding circuits given by Fig. 1.(b), which is a combination of CNOT and  $Z$ -rotation gate. The 3-body terms in the Hamiltonian which is expressed by  $H_{C3} = \sum_{j < k < m} c_{jkm} \hat{\sigma}_j^z \hat{\sigma}_k^z \hat{\sigma}_m^z$  has a corresponding circuits given by Fig. 1.(c), which is a combination of CNOT and  $Z$ -rotation gate acting on 3 qubits. Finally, a 4-body terms in the Hamiltonian  $H_{C4} = \sum_{j < k < m < n} c_{jkmn} \hat{\sigma}_j^z \hat{\sigma}_k^z \hat{\sigma}_m^z \hat{\sigma}_n^z$  has a corresponding circuits given by Fig.1.(d), which is a combination of CNOT and  $Z$ -rotation gate acting on 4 qubits. This figure also display a 1-layer quantum circuit of 12-order QAOA WBH and 44-order QAOA Turyn methods constructed from 1-, 2-, 3-, and 4- body terms circuits; displayed in (e) and (f) respectively, which will be discussed in more detail in the following sections.

### 3 Experiments

We do the experiments using both of simulators and quantum hardware. In the latest case, we implement simple experiment on low qubit number of IBM quantum computer. Before implementing the quantum circuit in Hadamard search, which involves several  $k$ -body interaction terms, we have tested its elementary circuits displayed in Fig.1 individually. The performance for each of these circuits are as expected, i.e., the distribution of solutions shows the validity of the circuit. Detail of the results can be found in the Supplementary Information,

The results of the algorithms discussed in this paper are in the form of  $L$ -length bit strings, so that there are  $2^L$  possible combination of them. A result is labelled as valid or correct when the value of the non-negative error/energy function related to the algorithm, i.e. the value of the Williamson or Turyn cost function, is equal to zero. Otherwise, it is labelled as wrong. To measure the performance of the algorithm in producing correct solutions, we can compare it to an algorithm that randomly generate every possible combination of an  $L$  length bit string. Therefore, for a given x-algorithm to measure, we propose xRAR (*x*-Algorithm to Random-Algorithm Ratio) as a performance metric.

The random algorithm generates  $2^L$  number of bit strings and we can evaluate whether each of the bit string is valid or not. When we know beforehand that there are  $S_R$  number of valid solutions among the  $2^L$  random bit strings, assuming a uniform probability distribution of the bit strings, the probability  $P_R$  to find a valid solution is  $P_R = \frac{S_R}{2^L}$ . On the other hand, the solutions generated by a quantum circuit that represents the x-algorithm are also probabilistic, and we can calculate the probability  $P_x$  of valid solution of the x-algorithm. Therefore, the value of xRAR; which conceptually is illustrated by Fig.2 (a), is given as follows

$$xRAR = \frac{P_x}{P_R} \quad (16)$$

The value of xRAR in Eq.(16) is a positive real number, where  $0 < xRAR < 1$  indicates that the x- algorithm is worse than the random algorithm  $R$ ,  $xRAR = 1$  it has a similar performance to the random algorithm, and  $xRAR > 1$  means that the x-algorithm is better than random algorithm  $R$ .

The execution steps of the QAOA in the experiments is displayed in Fig.2 (b). When running the quantum algorithm, either in a simulator or in a real quantum computer, we repeat the run  $N$  times, which is called as the number of shots. It yields  $N$  number of solutions/bit strings and its corresponding energy/error. A particular block/part of the algorithm will calculate the average or expectation, where we also can check whether particular bit strings or

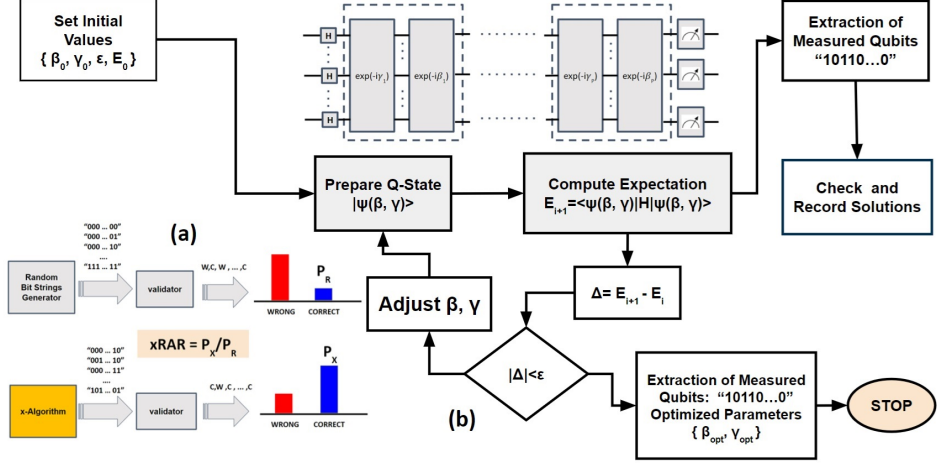


Figure 2: Workflow diagram and performance metric: (a) Performance Measure in Term of xRAR. The probability  $P_x$  of correct or valid answers of the x-algorithm that generates  $L$ -length bit strings is compared to  $P_R$ , which is the correct probability of a random algorithm that generates  $L$ -length (uniform) randomly distributed bit strings., (b) The QAOA processing steps.

solution achieve a minimum energy shown as the block *Extraction of Measured Qubits* in the figure. We can count the number of the valid solution in each iteration step and after the lowest average energy for a particular experiment setup is achieved. The number of correct solutions can be used for determining the performance of the algorithm.

In addition to XRAR, we also evaluate the performance of the algorithm with an error metric. This error metric is accumulated or total objective values of all generated solutions, with the objective measure are given by either the Williamson or Turyn cost functions given by Eq.(3) and Eq.(6), respectively. The value is normalized by the maximum of each cost function, then compared to the value of random algorithm which is calculated by exhaustive search. Therefore, for a particular order of H-SEARCH that generates  $N_Q$ -length bit string solution with maximum objective error of  $E_{max}$  and total error for all possible  $2^{N_Q}$ -bit string equal to  $E_{tot}$ , we have normalization factor  $E_{max}2^{N_Q}$ , the average error of  $E_{tot}/2^{N_Q}$ , and normalized average error of  $E_{tot}/(2^{N_Q}E_{max})$ . The normalized average error is used to compare the performance of algorithms with various number of shots (sampling).

The lowest order case for the Williamson method is 12, which corresponds to 36-order Baumert-Hall H-matrix, requires 8 qubits to implement. The energy function of this problems was obtained similarly to our previous paper [24].

An exhaustive search to all possible  $2^8$  bit strings that yields minimum energy; and therefore correct bit strings, found 64 WBH-sequences as valid solutions. This result yields the probability value to find the solution of 8-length uniformly distributed bit strings  $P_R = \frac{1}{4}$ ; therefore, the maximum QRAR performance is  $\frac{1}{P_R} = 4$ . It is also found that the maximum value of the cost function is 18 and the total error of 1024; therefore, the normalized average error is equal to 0.2222. The Hamiltonian of this problem is given by

$$\hat{H}(\hat{\sigma}) = 2\hat{\sigma}_0^z\hat{\sigma}_1^z + 2\hat{\sigma}_2^z\hat{\sigma}_3^z + 2\hat{\sigma}_4^z\hat{\sigma}_5^z + 2\hat{\sigma}_6^z\hat{\sigma}_7^z + \hat{\sigma}_0^z\hat{\sigma}_1^z\hat{\sigma}_2^z\hat{\sigma}_3^z + \hat{\sigma}_0^z\hat{\sigma}_1^z\hat{\sigma}_4^z\hat{\sigma}_5^z + \hat{\sigma}_0^z\hat{\sigma}_1^z\hat{\sigma}_6^z\hat{\sigma}_7^z + \hat{\sigma}_2^z\hat{\sigma}_3^z\hat{\sigma}_4^z\hat{\sigma}_5^z + \hat{\sigma}_2^z\hat{\sigma}_3^z\hat{\sigma}_6^z\hat{\sigma}_7^z + \hat{\sigma}_4^z\hat{\sigma}_5^z\hat{\sigma}_6^z\hat{\sigma}_7^z + 4 \quad (17)$$

Note that in the minimization, the constant term can be dropped without affecting the result. We will do some experiments for this case with both of the simulator and real quantum computer.

First, we run the QAOA-HSEARCH algorithm in a quantum computer simulator (IBM-Qiskit) with various number of layers, random initialization of  $\{\beta_0, \gamma_0\}$  parameters, and using

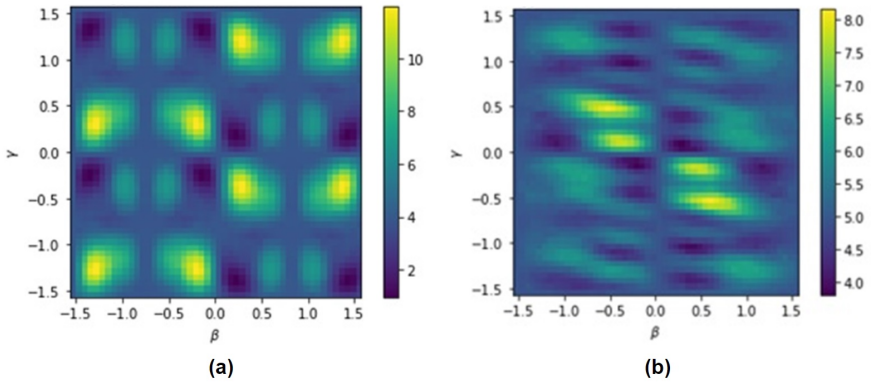


Figure 3: Comparisons of lowest order PEL (Potential Energy Landscape): (a) 12-order QAOA-Williamson and (b) 44-order QAOA-Turyn

COBYLA (Constrained Optimization BY Linear Approximation) which is available in the Python library for optimization [29]. Figure 1 (d) shows a one-layer quantum circuit related to Eq.(17).

The energy distribution as a function of  $\gamma$  and  $\beta$  parameters displayed as PEL (Potential Energy Landscape) in Fig.3 shows a periodic landscape, with minima located around the first (right upper part) and third quadrants (left lower part). Fig.4 (a) shows the performance of the algorithm with the number of layers  $p$  are increased stepped wisely, i.e,  $p = 1, \frac{NQ}{2}, NQ, 2NQ, 4NQ$ . Considering the location of the minima which are indicated in the PEL, the initialization of the parameters have been picked up within  $(-0.5, 0.5)$  interval. We repeat the experiment 10 times and plot the mean value of XRAR and Error in the figure. We observed that the value of xRAR consistently increased asymptotically to its maximum theoretical value of  $XRAR = 4$  at  $p = 4NQ = 32$ . At the same time, we observed that increasing the number of layer reduces the error. The resulting 12-order of the Williamson's and its corresponding 36 order of Baumert-Hall's are displayed in Fig. 5 (a) and Fig. 5 (b), respectively.

We also implemented the algorithm of finding 12-order Williamson matrix in a quantum computer hardware. An IBM quantum computer, in this case is the IBM-Brisbane machine powered by a 127 qubits Eagle r.3 of version 1.1.6 quantum processor, was employed. The processor's qubits mean coherence time are  $T_1 \approx 227\mu s, T_2 \approx 130\mu s$  with median ECR error  $\approx 7 \times 10^{-3}$  and median SX error  $\approx 2 \times 10^{-4}$ . We also repeat the run 10 times and the number of shots in the hardware is set to 1024. The results is displayed in Fig. 4(b), which is the quantum hardware (QPU) performance for the QAOA 12-order Williamson method with number of layers 1, 2, 3 and 4. This figure shows that although the mean error of QAOA implemented on hardware (blue dotted line with "x" symbols) are consistently lower than the mean error of random algorithm (blue dotted line in the upmost part), the mean XRAR performance (red solid line with red circle symbols) is sometimes only slightly better than the random algorithm bound (red solid line) for number of layer of 1 and 3, and worse for 2 and 4. Since initialization of the angle can influence the final results, in term of XRAR, we also display the maximum XRAR for each repeated 10 times run. The max RAR performance initially higher than random but then tend to decrease when the number of layers are increased. This shows the circuit depth enlarge noise in the qubits.

In the Turyn-based method, for a particular order of H-matrix that we want to construct, we have to find a corresponding TT (Turyn Type)-Sequence [16, 21, 25, 24]. In term of previously formulated energy function in Eq.(6), we are looking for a T-string  $\vec{s}$ . For even positive integers  $N = 4, 6, 8, \dots$ , the order of related Turyn's Hadamard matrix will be  $M = 4(3N - 1)$  and the number of variables or required qubits is  $Q = 4N - 11$ . We will do experiments for  $N = 4, 6, 8$  that corresponds to order  $M = 44, 68, 92$  which requires  $Q = 5, 13, 21$  qubits.

In the first experiment, we want to find a Turyn H-matrix of order-44 which needs 5 qubits. The problem Hamiltonian is given by the following expression,

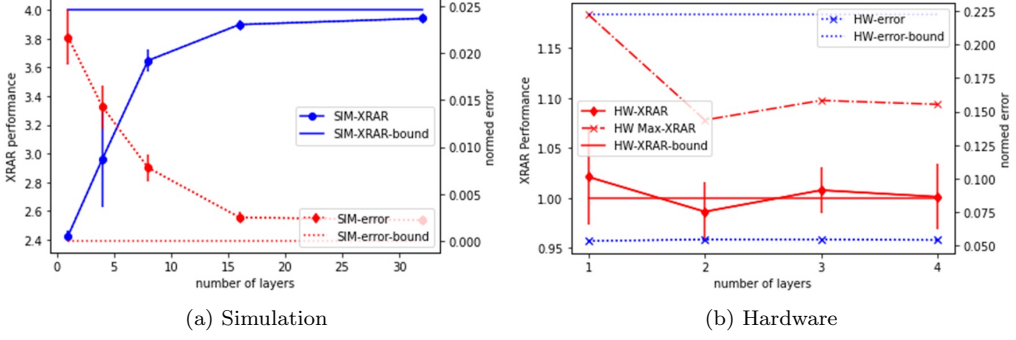


Figure 4: Performance of 12-Williamson/36-Baumert Hall QAOA Methods. Fig. (a) displays simulation results: solid blue line with blue circles is the XRAR, solid blue line is the upper bound of XRAR which is equal to 4, red-dotted line with circle is the normalized objective error, dotted line is the lower bound of error which is equal to zero. Fig. (b) Shows the hardware performance: dotted blue line with  $\times$  symbols is the objective error, dotted blue line at the upper part is the error threshold for random algorithm, solid red line with circle is the mean XRAR, solid red line is the XRAR of random algorithm, and the red dashed-dot with  $\times$  symbols are maximum value of XRAR at corresponding layer number

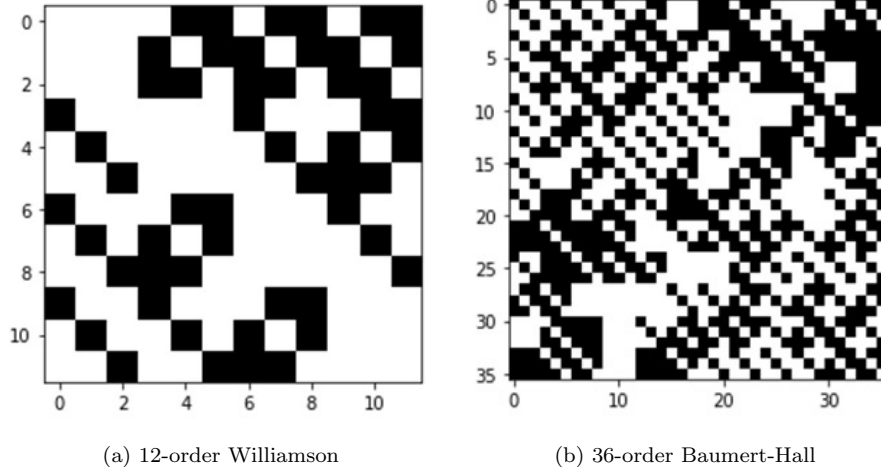


Figure 5: The 12-order Williamson/36-order Baumert-Hall Hadamard Matrices found by the algorithms. Both simulation and hardware found identical H-matrices.

$$\begin{aligned}
 \hat{H}(\hat{\sigma}) = & \hat{\sigma}_0^z \hat{\sigma}_1^z \hat{\sigma}_2^z + \hat{\sigma}_0^z \hat{\sigma}_3^z \hat{\sigma}_4^z + \hat{\sigma}_0^z \hat{\sigma}_3^z - \hat{\sigma}_0^z \hat{\sigma}_4^z + \hat{\sigma}_1^z \hat{\sigma}_2^z \hat{\sigma}_3^z \hat{\sigma}_4^z \\
 & + \hat{\sigma}_1^z \hat{\sigma}_2^z \hat{\sigma}_3^z + 2\hat{\sigma}_1^z \hat{\sigma}_2^z + \hat{\sigma}_1^z \hat{\sigma}_3^z \hat{\sigma}_4^z + \hat{\sigma}_1^z \hat{\sigma}_3^z + \hat{\sigma}_1^z \hat{\sigma}_4^z + \hat{\sigma}_1^z + \hat{\sigma}_2^z \hat{\sigma}_3^z \hat{\sigma}_4^z \\
 & + \hat{\sigma}_2^z \hat{\sigma}_3^z + \hat{\sigma}_2^z \hat{\sigma}_4^z + \hat{\sigma}_2^z + \hat{\sigma}_4^z + 5
 \end{aligned} \tag{18}$$

The corresponding quantum circuit can be constructed automatically using a construction algorithm, which the one layer circuit is shown in Fig. 1 (f). We then run the QAOA on both of quantum simulator and quantum hardware, which successfully found the 44-order Turyn H-matrix. As shown in the QAOA flowchart in Fig. 2, normally we need to put the process done in the quantum computing inside the optimization, so that an exclusive access to this device is

mandatory. However, since we used a public access to 5 qubits IBM quantum computer, such dedicated access was not permitted. Therefore, we only implemented the optimized quantum circuits obtained in the simulation into the 5 qubits IBM Quito.

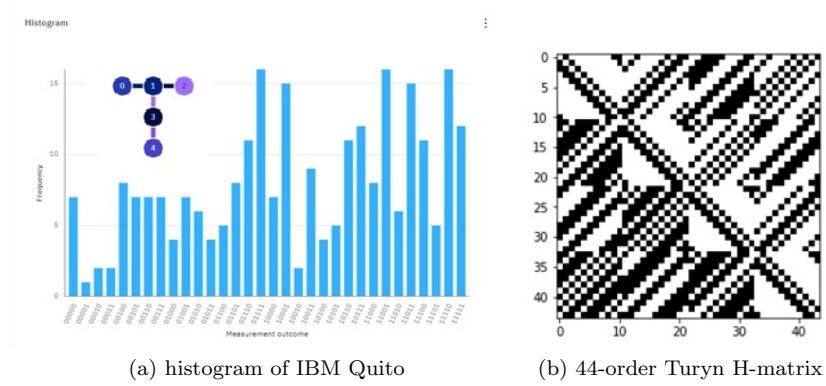


Figure 6: Results for 44-order Turyn Method

The 44-order H matrix for both of the simulator and hardware are identical, which is shown in Fig. 6: (a) implementation in IBM-Quito, and (b) obtained order-44 of the Turyn H-matrix. The histogram indicates that the number of the valid solution, i.e. the bit string "11100", is equal to 11; which means that it consists of about 6% correct solution. Since random algorithm would have yield only 3.1%, the quantum processor indicates a little bit more advantage than the classical.

The PEL of the QAOA for high order H-matrices are more rough than the lower ones shown previously, implying that selection of initial parameters is both difficult and crucial. In this subsection, we show the results of finding 44-order Williamson/132-order Baumert-Hall matrices. We use only 1-layer and choose various initialization parameters. The number of required qubits to implement is 24. After setting the number of sampling to 10,000 shots, we obtained the mean xRAR on 10 different parameter initialization is equal to 1.14 with the maximum value of 3.50. One of the obtained matrix is displayed in Fig. 7, where (a) shows 44-order Williamson and (b) the 132-order Baumert-hall matrices.

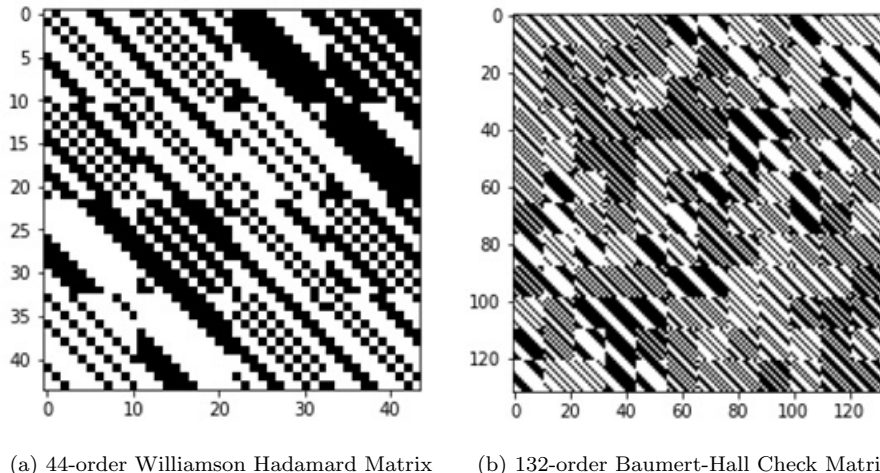


Figure 7: Experiment Results of Simulator and Quantum Hardware: (a) Williamson Matrix of Order 44 and (b) Baumert-Hall of Order 132

## 4 Discussion

We have shown a possibility to implement a Hadamard matrix searching method on a quantum computer simulator. Experiments on a quantum computer simulator shows an exponential improvement of the QAOA-based quantum algorithm over random search algorithm. At the final stage, we have run and find a 44-order Williamson or 132-order Baumert-Hall matrices successfully.

## Acknowledgments

This work has been supported partially by the P2MI Program of STEI-ITB and by the Blueqat Inc., Tokyo, Japan.

## Competing interests

The authors declare no competing interests.

## Author contributions statement

A.B.S formulated the theory, conducted the experiment(s), analyzed the results, and writing of the paper.

## Data and Codes Availability

All of codes and data will be provided upon direct request to the authors. Some parts of the codes will be made available for public upon publication of the manuscript.

## References

- [1] F. Arute et al. Quantum supremacy using a programmable superconducting processor. *Nature*, 574(7779):505–510, 2019.
- [2] E. Farhi, J. Goldstone, and S. Gutmann. A quantum approximate optimization algorithm. *arXiv e-prints*, page 1411.4028, 2014.
- [3] S. Boulebnane, X. Lucas, A. Meyder, S. Adaszewski, and A. Montanaro. Peptide conformational sampling using the quantum approximate optimization algorithm. *NPJ Quantum Information*, 9(70), 2023.
- [4] Z. He, R. Shaydulin, S. Chakrabarti, D. Herman, C. Li, Y. Sun, and M. Pistoia. Alignment between initial state and mixer improves qaoa performance for constrained optimization. *NPJ Quantum Information*, 9(121), 2023.
- [5] L. Cheng, YQ. Chen, SX. Zhang, and S. Zhang. Quantum approximate optimization via learning-based adaptive optimization. *Communications Physics volume*, 7(83), 2024.
- [6] H. Jing, Y. Wang, and Y. Li. Data-driven quantum approximate optimization algorithm for power systems. *Comm. Engineering*, 2(12), 2023.
- [7] Y. Kim, A. Eddins, S. Anand, K.X. Wei, E. van den Berg, S. Rosenblatt, H. Nayfeh, Y. Wu, M. Zaletel, K. Temme, and A. Kandala. Evidence for the utility of quantum computing before fault tolerance. *Nature*, pages 500–505, 2023.
- [8] J. Hadamard. Resolution d'une question relative aux determinants. *Bull. des Sciences Math.*, 2:240–246, 1893.
- [9] J.J. Sylvester. Thoughts on inverse orthogonal matrices, simultaneous sign successions, and tessellated pavements in two or more colours, with applications to Newton's rule, ornamental tile-work, and the theory of numbers. *Philos. Mag.*, 34(232):461–475, 1867.
- [10] V. Garg. *Wireless Communications and Networking*. Princeton University Press, 2007.
- [11] K.J. Horadam. *Hadamard Matrices and Their Applications*. Princeton University Press, 2007.
- [12] A. Hedayat and W.D. Wallis. Hadamard matrices and their applications. *Ann. Stat.*, 6(6):1184–1238, 1978.
- [13] R.E.A.C. Paley. On orthogonal matrices. *J. Math. Phys.*, 12(1-4):311–320, 1933.
- [14] J. Williamson et al. Hadamard's determinant theorem and the sum of four squares. *Duke Math. J.*, 11(1):65–81, 1944.
- [15] L. Baumert and M. Hall. A new construction for Hadamard matrices. *Bull. Amer. Math. Soc.*, 71(1):169–170, 1965.
- [16] R.J. Turyn. Hadamard matrices, Baumert-Hall units, four-symbol sequences, pulse compression, and surface wave encodings. *J. Comb. Theory Ser. A*, 16(3):313–333, 1974.
- [17] K.J. Horadam. Cocyclic development of designs. *J. Algebraic Combin.*, (2), 1993.
- [18] K.J. Horadam and W. de Launey. Generation of cocyclic hadamard matrices. *Math. Appl.*, 325, 1995.
- [19] K.J. Horadam. An introduction to cocyclic generalised hadamard matrices. *Discrete Applied Mathematics*, (102), 2000.
- [20] J.A. Alvarez, V. and Armario, M.R. Falcon, F. Frau, M.D. and Gudiel, M.B. Guemes, and A. Osuna. On cocyclic hadamard matrices over goethals-seifel loops. *Mathematics*, 8(24), 2020.
- [21] H. Kharaghani and B. Tayfeh-Rezaie. A Hadamard matrix of order 428. *J. Comb. Des.*, 13(6):435–440, 2005.
- [22] A.B. Suksmono. Finding a hadamard matrix by simulated quantum annealing. *Entropy*, 20(2), 2018.
- [23] A.B. Suksmono and Y. Minato. Finding Hadamard matrices by a quantum annealing machine. *Sci. Rep.*, 9:14380, 2019.

- [24] A.B. Suksmono and Y. Minato. Quantum computing formulation of some classical hadamard matrix searching methods and its implementation on a quantum computer. *Scientific Reports*, yy(xx), 2022.
- [25] S. London. *Constructing New Turyn Type Sequences, T-Sequences and Hadamard Matrices*. PhD thesis, University of Illinois at Chicago, 2013.
- [26] M.A. Nielsen and I.L. Chuang. *Quantum Computation and Quantum Information*. Cambridge Univ. Press, 2010.
- [27] J.T. Seeley, M.J. Richard, and P. Love. The bravyi-kitaev transformation for quantum computation of electronic structure. *arXiv*, page 1208.5986, 2012.
- [28] K. Setia and J.D. Whitfield. Bravyi-kitaev superfast simulation of electronic structure on a quantum computer. *arXiv*, page 1712.00446, 2018.
- [29] M. J. D Powell. A direct search optimization method that models the objective and constraint functions by linear interpolation. *Mathematics and Its Applications*, 275:51–67, 1994.